Synthesis and Stereoisomerism of [*n*]Cyclo-2,9-phenanthrenylene Congeners Possessing Alternating *E*/*Z*- and *R*/*S*-Biaryl Linkages

Journal:	*Organic & Biomolecular Chemistry*
Manuscript ID	OB-ART-05-2020-001064.R1
Article Type:	Paper
Date Submitted by the Author:	13-Jun-2020
Complete List of Authors:	Yang, Yong; The University of Tokyo, Department of Chemistry Nanjo, Yuki; The University of Tokyo, Department of Chemistry Isobe, Hiroyuki; The University of Tokyo, Department of Chemistry Sato, Sota; The University of Tokyo, Department of Chemistry

ARTICLE

Synthesis and Stereoisomerism of [*n*]Cyclo-2,9-phenanthrenylene Congeners Possessing Alternating *E*/*Z*- and *R*/*S*-Biaryl Linkages

Yong Yang,[ab] Yuki Nanjo,[a] Hiroyuki Isobe[ab] and Sota Sato*[ab]

Received 00th January 20xx,
Accepted 00th January 20xx

DOI: 10.1039/x0xx00000x

www.rsc.org/

The synthesis and cyclostereoisomerism of [*n*]cyclo-2,9-phenanthrenylenes ([*n*]CPhen$_{2,9}$, *n* = 4, 6 and 8), possessing hybrid *E*/*Z*- and *R*/*S*-biaryl linkages, were elaborated. The dimer of a phenanthrene derivative was used as a starting material and underwent Ni-mediated Yamamoto-type coupling to afford [6]CPhen$_{2,9}$ as a major cyclic product, as well as [4]CPhen$_{2,9}$ and [8]CPhen$_{2,9}$ as minor products. The stereoisomers of [*n*]CPhen$_{2,9}$ were isolated and characterized, and the number of stereoisomers indicated that *E*/*Z* linkages did not provide any experimentally separable isomer, whereas the chirality in [*n*]CPhen$_{2,9}$ originated from the intrinsic axial chirality at constrained *R*/*S* linkages. Theoretical calculations predicted that the 2,2′-linkages in [*n*]CPhen$_{2,9}$ adopted a fixed *Z*- or *E*-configuration, which suggested a novel type of dynamics of atropisomerism in contrast to the reported rigid or flexible behavior. This study enriches our understanding of the stereochemical features of *E*/*Z* linkages in aromatic macrocycles.

Introduction

Events in molecules take place in three dimensions, and when describing the three-dimensional structures of molecules, stereochemistry deepens our understanding of molecular science. [1] Among various forms of stereoisomerism, atropisomers in biaryl systems are unique, as stereoisomers emerge in the absence of chiral centers.[2] After the discovery of stereoisomers of biphenyls in 1922,[3] a variety of molecules with biaryl atropisomerism facilitated the development of modern chemistry, such as asymmetric catalysts.[4] The chirality at biaryl linkages is typically recognized with *R*/*S* configurations at twisted sp^2-sp^2 C–C bonds,[5] which also gives rise to the unique cyclostereoisomerism of cyclic molecules. [6] Cyclostereoisomerism has been found to be unique and complex, involving another *E*/*Z* configuration at planar sp^2-sp^2 C–C bonds (Fig. 1).[7] After the first example of [4]cyclo-2,8-chrysenylene ([4]CC$_{2,8}$) composed solely of *E*/*Z*-biaryl linkages, [8,9] *E*/*Z*-cyclostereoisomerism was further revealed by the design and synthesis of serial congeners of [*n*]cyclo-*amphi*-naphthylenes ([*n*]CaNAP) with naphthylene panels of *n* = 6–11. [10] The structural rigidity of the *E*/*Z*-linkers depended on the ring size, and stereoisomerism did not persist under ambient conditions. Cyclostereoisomerism was further diversified by one peculiar cycloarylene, [8]cyclo-3,9-phenanthrenylene ([8]CPhen$_{3,9}$). [11] This molecule possessed alternating *E*/*Z*- and *R*/*S*-biaryl linkages, and the stereoisomerism became more unique and perplexing. Although this peculiar example demonstrated the existence of a mixed stereoisomerism, the in-depth chemistry, such as size dependency, was not fully appreciated.

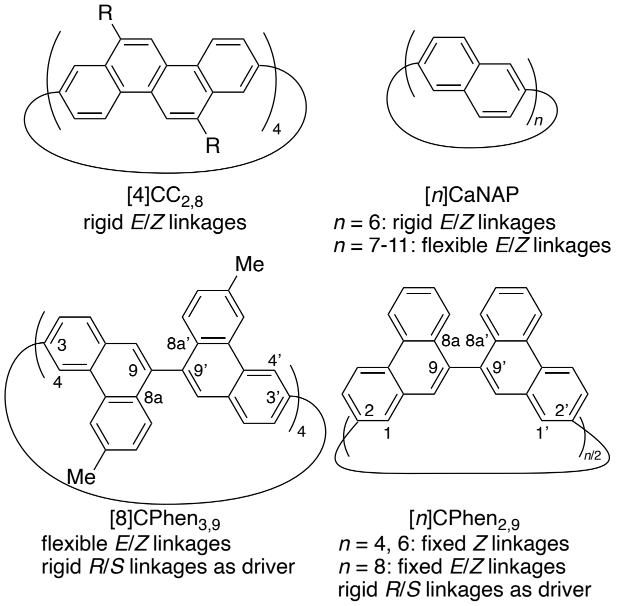

[4]CC$_{2,8}$
rigid *E*/*Z* linkages

[*n*]CaNAP
n = 6: rigid *E*/*Z* linkages
n = 7-11: flexible *E*/*Z* linkages

[8]CPhen$_{3,9}$
flexible *E*/*Z* linkages
rigid *R*/*S* linkages as driver

[*n*]CPhen$_{2,9}$
n = 4, 6: fixed *Z* linkages
n = 8: fixed *E*/*Z* linkages
rigid *R*/*S* linkages as driver

Fig. 1. Structures of cycloarylenes with *E*/*Z* geometries.

In this work, we explored mixed cyclostereoisomerism through the synthesis of a series of [*n*]cyclo-2,9-phenanthrenylenes ([*n*]CPhen$_{2,9}$, *n* = 4, 6 and 8, Fig. 1). The molecules possess *E*/*Z*- and *R*/*S*-biaryl linkages at the 2,2′- and 9,9′-connections, respectively, which give rise to serial congeners with alternating *E*/*Z* and *R*/*S* linkages. The [*n*]CPhen$_{2,9}$ congeners were not only unique in their stereoisomerism but also rich in structural chemistry, including interesting molecular packing in crystals. The

---

[a] *Department of Chemistry, The University of Tokyo, Hongo, Bunkyo-ku, Tokyo 113-0033, Japan. E-mail: satosota@appchem.t.u-tokyo.ac.jp*
[b] *JST, ERATO, Isobe Degenerate π-Integration Project, Hongo, Bunkyo-ku, Tokyo 113-0033, Japan*

† Electronic Supplementary Information (ESI) available: Supplementary data and methods. CCDC 1977015, 1976911 and 1976912. For ESI and crystallographic data in CIF or other electronic formats, see DOI: 10.1039/x0xx00000x

cyclostereoisomerism reported in this study represents a novel type of stereochemical dynamics in cycloarylenes with rigid *R*/*S* linkages and fixed *E*/*Z* linkages.

Results and discussion

Synthesis

We synthesized [*n*]CPhen$_{2,9}$ through Ni-mediated Yamamoto-type coupling of dimeric phenanthrene compound **1**. As shown in Scheme 1 and Scheme S1 in ESI, commercially available 2-iodophenylacetic acid underwent Perkin condensation with 3-bromobenzaldehyde to provide compound **2** in 90% yield. Notably, **2** predominantly adopted the *Z*-configuration, as characterized by single-crystal X-ray structure analysis. The next $K_2S_2O_8$/H_2SO_4–promoted oxidative cyclization[12] of **2** resulted in 2-bromo-9-phenanthrenecarboxylic acid (**3**) in 80% yield. Photochemical conversion with 1,3-diiodo-5,5-dimethylhydantoin was applied to accomplish the iodination to produce 2-bromo-9-iodophenanthrene (**4**) in 55% yield. The subsequent Suzuki-Miyaura coupling gave 9,9′-biphenanthrenyl derivative **1** in 55% yield, which served as a starting material and was subjected to the final macrocyclization. Ni-mediated Yamamoto-type coupling afforded [6]CPhen$_{2,9}$ as a major cyclic product in 24% yield, along with [4]CPhen$_{2,9}$ and [8]CPhen$_{2,9}$ as minor products in 3% and 8% yield, respectively.[13] Astoundingly, [4]CPhen$_{2,9}$ was unexpectedly generated. To the best of our knowledge, tetrameric congeners of cyclo-*meta*-arylenes[14] have rarely been achieved or even detected in the literature.[15,16,17,18] We speculated that the severe steric repulsion derived from 1,1′-binaphthyl linkages (8a-9-9′-8a′, Fig. 1) contributed to the formation of a tetrameric macrocycle.

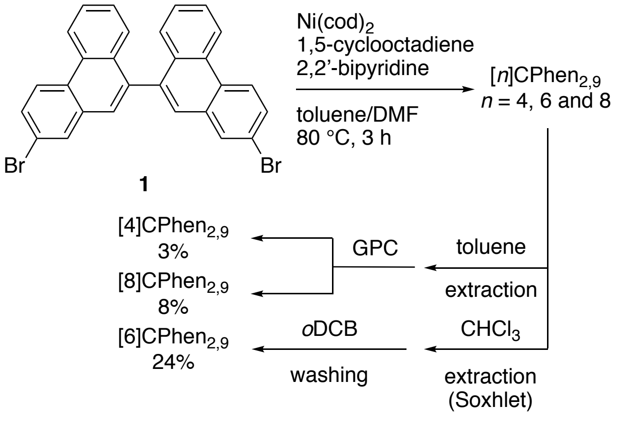

Scheme 1. Synthesis of [*n*]CPhen$_{2,9}$.

Stereoisomers, separation and crystal structures

[6]CPhen$_{2,9}$ consists of three 2,2′-binaphthyl and three 1,1′-binaphthyl linkages with *E*/*Z*- and *R*/*S*-configurations, respectively. A coalescent consideration of *E*/*Z*- and *R*/*S*-configurations gives rise to 20 stereoisomers comprising 10 diastereomers and 10 enantiomer pairs (see Table S1 in ESI). In comparison, consideration of solely *R*/*S* configurations results in four stereoisomers comprising two diastereomers and two enantiomer pairs (Fig. 2d). As shown in Fig. 2a, we successfully separated four stereoisomers of [6]CPhen$_{2,9}$ (Fr. 1–4) with preparative HPLC. Identical NMR spectra (see Fig. S10 in ESI) and mirror CD images (Fig. 2e,f) were found for Fr. 1/2 and Fr. 3/4, indicative of the presence of enantiomeric pairs for Fr. 1/2 and Fr. 3/4. The number of ^{1}H NMR resonances was 8 for Fr. 1/2 and 24 for Fr. 3/4, suggesting the (*S*,*S*,*S*)*- and (*S*,*S*,*R*)*-configurations[19] at 1,1′-binaphthyl linkages in [6]CPhen$_{2,9}$, respectively. Therefore, four stereoisomers, including two diastereomers and two enantiomer pairs, were experimentally isolated, in good accordance with the result of mathematical counting with consideration of solely *R*/*S* configurations. In this way, we concluded that 2,2′-binaphthyl linkages did not afford any experimentally separable isomer because the 2,2′-linkages in [6]CPhen$_{2,9}$ were flexible or fixed to *E*- or *Z*-configuration. We then elucidated the dynamic behavior of 2,2′-linkages in (*S*,*S*,*S*)-[6]CPhen$_{2,9}$ by scan calculations with the semiempirical PM6 method (Fig. 2b), and found that one energy minimum point (hereafter denoted as a "stationary point") arose in the *Z*-configuration, whereas no stationary point arose in the *E*-configuration. This result implied that the 2,2′-linkage in (*S*,*S*,*S*)-[6]CPhen$_{2,9}$ was fixed to *Z*-configuration rather than fluctuating between *E*- and *Z*-configurations. *E*/*Z* atropisomerism at biaryl linkage in reported cycloarylenes showed two types of dynamic behavior: rigid and flexible (Fig. 2c).[6] For either *E*- or *Z*-configuration, one stationary point exists, and the *E* and *Z* configurations at biaryl linkages are rigid with a high energy barrier of over 20 kcal/mol, while they are flexible with a low energy barrier of 5–20 kcal/mol, according to the IUPAC definition.[20] The fixed *E*/*Z*-biaryl linkages found in (*S*,*S*,*S*)-[6]CPhen$_{2,9}$ represented a third type of dynamics of atropisomerism (Fig. 2c). In the same manner, 2,2′-linkages adopted a fixed *Z*-configuration in (*S*,*S*,*R*)-[6]CPhen$_{2,9}$ (see Fig. S12 in ESI). Therefore, the four isolated stereoisomers were eventually assigned as (*Z*,*S*,*Z*,*S*,*Z*,*S*)-, (*Z*,*R*,*Z*,*R*,*Z*,*R*)-, (*Z*,*S*,*Z*,*S*,*Z*,*R*)- and (*Z*,*R*,*Z*,*R*,*Z*,*S*)-[6]CPhen$_{2,9}$. The density functional theory (DFT) calculations at the B3LYP/6-31G(d,p) level of theory suggested that (*Z*,*S*,*Z*,*S*,*Z*,*S*)*-[6]CPhen$_{2,9}$ was more stable than (*Z*,*S*,*Z*,*S*,*Z*,*R*)*-[6]CPhen$_{2,9}$ by 3.4 kcal/mol (Fig. 2d). The absolute configurations for (*Z*,*S*,*Z*,*S*,*Z*,*S*)/(*Z*,*R*,*Z*,*R*,*Z*,*R*)-[6]CPhen$_{2,9}$ (Fr. 1/2) and (*Z*,*S*,*Z*,*S*,*Z*,*R*)/(*Z*,*R*,*Z*,*R*,*Z*,*S*)-[6]CPhen$_{2,9}$ (Fr. 3/4) were clarified with CD spectroscopy and the time-dependent DFT (TD DFT) method at the B3LYP/6-31G(d,p) level of theory (Fig. 2e,f). The CD spectra showed mirror images for Fr. 1/2 and 3/4, and TD DFT calculations predicted the theoretical spectra of (*Z*,*R*,*Z*,*R*,*Z*,*R*)- and (*Z*,*R*,*Z*,*R*,*Z*,*S*)-[6]CPhen$_{2,9}$. By matching the experimental and theoretical spectra, Fr. 2 was determined as (*Z*,*R*,*Z*,*R*,*Z*,*R*)-[6]CPhen$_{2,9}$, and Fr. 3 was determined as (*Z*,*R*,*Z*,*R*,*Z*,*S*)-[6]CPhen$_{2,9}$, consequently resulting in the assignment of Fr. 1 as (*Z*,*S*,*Z*,*S*,*Z*,*S*)-[6]CPhen$_{2,9}$ and Fr. 4 as (*Z*,*S*,*Z*,*S*,*Z*,*R*)-[6]CPhen$_{2,9}$.

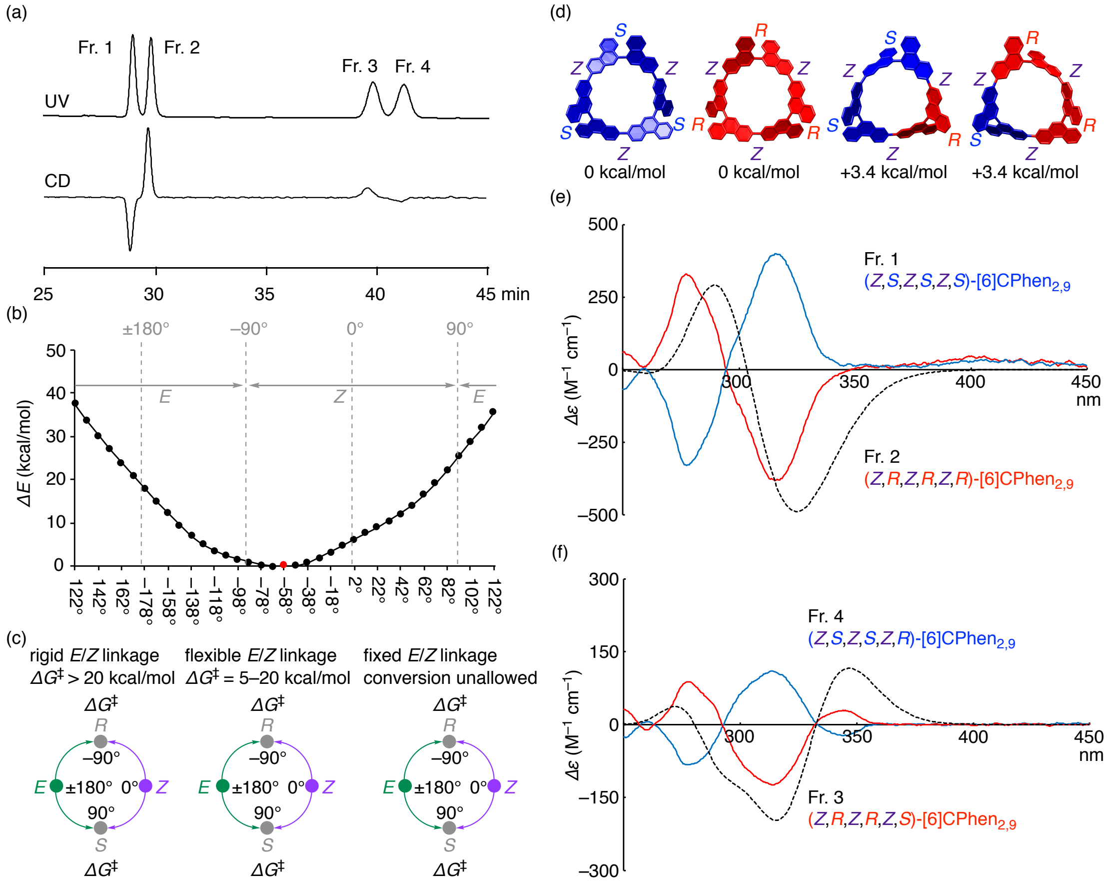

Fig. 2. Analysis of [6]CPhen$_{2,9}$. (a) Chiral HPLC separation of [6]CPhen$_{2,9}$ using a Daicel Chiralpak IA column. (b) Energy profile of the 2,2′-linkage (1-2-2′-1′) in (*E*/*Z*,*S*,*Z*,*S*,*Z*,*S*)-[6]CPhen$_{2,9}$ from scan calculations. The red dot shows a stationary point. (c) Relationship between dynamic behavior and thermodynamics at the *E*/*Z* biaryl linkage. The degrees are the dihedral angles at the biaryl linkage. (d) Structures and energetics of isolated stereoisomers of [6]CPhen$_{2,9}$. CD spectra of (e) (*Z*,*S*,*Z*,*S*,*Z*,*S*)/(*Z*,*R*,*Z*,*R*,*Z*,*R*)-[6]CPhen$_{2,9}$ and (f) (*Z*,*S*,*Z*,*S*,*Z*,*R*)/(*Z*,*R*,*Z*,*R*,*Z*,*S*)-[6]CPhen$_{2,9}$ in chloroform at 25 °C. The dotted curves are theoretical CD spectra of (e) (*Z*,*R*,*Z*,*R*,*Z*,*R*)-[6]CPhen$_{2,9}$ and (f) (*Z*,*R*,*Z*,*R*,*Z*,*S*)-[6]CPhen$_{2,9}$.

Adapted from the discussion of [6]CPhen$_{2,9}$, we explored [4]CPhen$_{2,9}$ in the same way. [4]CPhen$_{2,9}$ consists of two 2,2′-binaphthyl and two 1,1′-binaphthyl linkages, and a mixture of *E*/*Z*- and *R*/*S*-configurations leads to 9 stereoisomers comprising six diastereomers and three enantiomer pairs (see Table S2 in ESI). In contrast, three stereoisomers consisting of two diastereomers and one enantiomer pair were provided with consideration of solely *R*/*S*-configurations. As shown in Fig. 3a, we succeeded in the separation of three stereoisomers of [4]CPhen$_{2,9}$ (Fr. 1–3) by the employment of preparative HPLC. The mirror CD images (Fig. 3c) were observed for Fr. 2/3, indicative of the presence of an enantiomeric pair, suggesting the (*S*,*S*)*-configuration at 1,1′-binaphthyl linkages in [4]CPhen$_{2,9}$. Therefore, Fr. 1 was expected to display (*S*,*R*)-configuration at 1,1′-binaphthyl linkages. The experimental achievement of two diastereomers and one enantiomer pair agreed with the statistical result with consideration of solely *R*/*S*-configurations. In this way, we summarized that 2,2′-binaphthyl linkages did not provide any experimentally separable isomer of [4]CPhen$_{2,9}$. Likewise, we then investigated the dynamic behavior of 2,2′-linkages in [4]CPhen$_{2,9}$ by scan calculations with the semiempirical PM6 method (see Fig. S13 in ESI), and found that the 2,2′-linkages adopted a fixed *Z*-configuration. As a result, Fr. 1 was determined to be (*Z*,*S*,*Z*,*R*)-[4]CPhen$_{2,9}$, and Fr. 2/3 were determined to be (*Z*,*S*,*Z*,*S*)- and (*Z*,*R*,*Z*,*R*)-[4]CPhen$_{2,9}$. DFT calculations at the B3LYP/6-31G(d,p) level of theory suggested that (*Z*,*S*,*Z*,*S*)*-[4]CPhen$_{2,9}$ was more stable than (*Z*,*S*,*Z*,*R*)-[4]CPhen$_{2,9}$ by 2.4 kcal/mol (Fig. 3b). The absolute configuration for (*Z*,*S*,*Z*,*S*)/(*Z*,*R*,*Z*,*R*)-[4]CPhen$_{2,9}$ (Fr. 2/3) was elucidated with CD spectroscopy and the TD DFT method at the B3LYP/6-31G(d,p) level of theory (Fig. 3c). The CD spectra showed mirror images for Fr. 2/3, and the TD DFT calculations predicted the theoretical spectrum of (*Z*,*R*,*Z*,*R*)-[4]CPhen$_{2,9}$. Upon matching the experimental and theoretical spectra, Fr. 2 and Fr. 3 were assigned to (*Z*,*S*,*Z*,*S*)- and (*Z*,*R*,*Z*,*R*)-[4]CPhen$_{2,9}$, respectively.

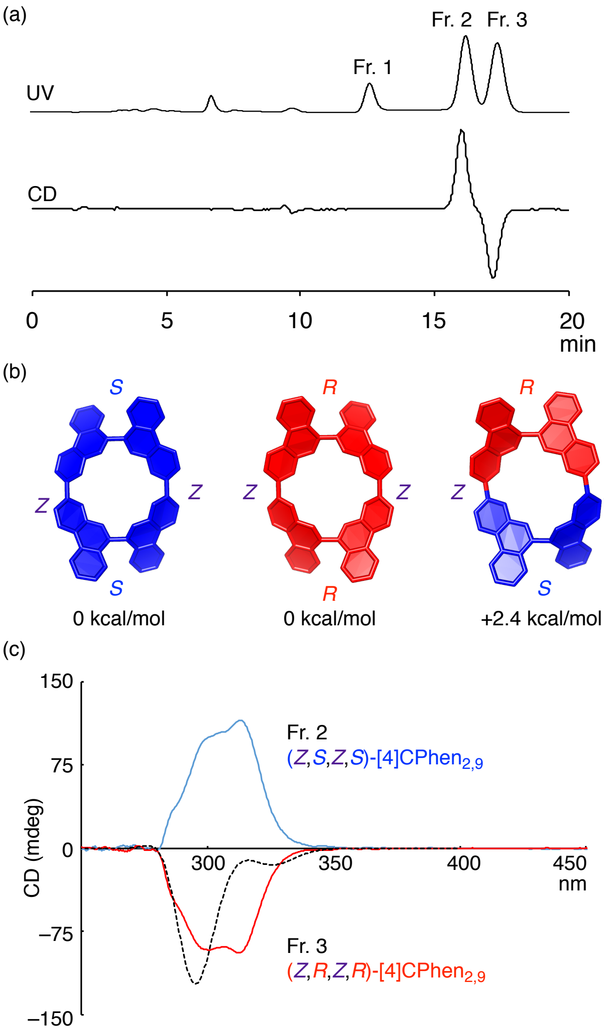

Fig. 3. Analysis of [4]CPhen$_{2,9}$. (a) Chiral HPLC separation of [4]CPhen$_{2,9}$ using a Cosmosil Cholester column. (b) Structures and energetics of isolated stereoisomers of [4]CPhen$_{2,9}$. (c) CD spectra of (*Z*,*S*,*Z*,*S*)/(*Z*,*R*,*Z*,*R*)-[4]CPhen$_{2,9}$ in chloroform at 25 °C. The dotted curve is the theoretical CD spectrum of (*Z*,*R*,*Z*,*R*)-[4]CPhen$_{2,9}$.

The stereochemistry of [8]CPhen$_{2,9}$ was intricate, with a large number of stereoisomers: there are 51 stereoisomers comprising 31 diastereomers and 20 enantiomer pairs when *E*/*Z*- and *R*/*S*-configurations are taken into account (see Table S3 in ESI). An overlook of *E*/*Z* configurations afforded six stereoisomers with four diastereomers and two enantiomer pairs. These statistical numbers were not consistent with the experimental result that only one isomer of [8]CPhen$_{2,9}$ was separated. To determine its structure, we performed large-scale low-mode conformational search calculations with molecular mechanics (MM3*) with 10000 steps and a maximum allowable closure distance of 30.0 Å to locate the possible candidates within 5 kcal/mol. As a result, 13 structures were predicted, and 9 stereoisomers were found after removal of the duplicates (see Table S4 in ESI). Among these, only (*Z*,*S*,*E*,*S*,*E*,*S*,*Z*,*R*)*-[8]CPhen$_{2,9}$ (Fig. 4) exhibited C_2 symmetry to afford ^{1}H NMR resonances that matched those of the isolated isomer. We performed DFT calculations of all 9 stereoisomers and found that the energy difference between (*Z*,*S*,*E*,*S*,*E*,*S*,*Z*,*R*)*-[8]CPhen$_{2,9}$ and the globally stable [8]CPhen$_{2,9}$ was 4.3 kcal/mol. Scan calculations predicted fixed *Z*- and *E*-configurations at 2,2′-linkages in (*Z*,*S*,*E*,*S*,*E*,*S*,*Z*,*R*)*-[8]CPhen$_{2,9}$ (see Fig. S14 in ESI). All the 2,2′-linkages in [4]CPhen$_{2,9}$ and [6]CPhen$_{2,9}$ adopted a fixed *Z*-configuration, whereas those in [8]CPhen$_{2,9}$ allowed fixed *E*-configuration in addition to fixed *Z*-configuration presumably because of the elevated structural flexibility led by the greater ring size of an octameric macrocycle. To further examine the presence of other [8]CPhen$_{2,9}$ stereoisomers, we heated (*Z*,*S*,*E*,*S*,*E*,*S*,*Z*,*R*)*-[8]CPhen$_{2,9}$ in 1,2,4-trichlorobenzene at 200 °C for hours but obtained an insoluble solid. We suspected that the separation of more stable isomers of [8]CPhen$_{2,9}$ was perturbed due to severely poor solubility.

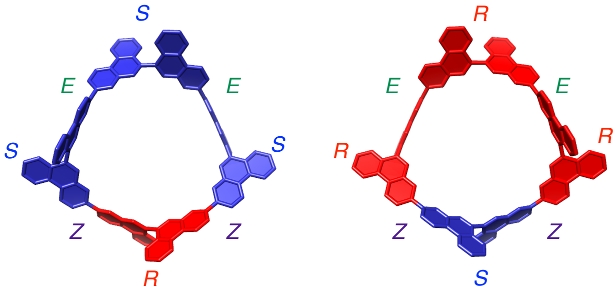

Fig. 4. Structures of (*Z*,*S*,*E*,*S*,*E*,*S*,*Z*,*R*)- and (*Z*,*R*,*E*,*R*,*E*,*R*,*Z*,*S*)-[8]CPhen$_{2,9}$.

We obtained qualified single crystals of (*Z*,*S*,*Z*,*S*,*Z*,*S*)*-[6]CPhen$_{2,9}$ and performed X-ray crystallographic analysis. As shown in Fig. 5a, the crystal structure of (*Z*,*S*,*Z*,*S*,*Z*,*S*)*-[6]CPhen$_{2,9}$ existed as a racemate. The dihedral angles measured with 3-2-2′-3′ carbon atoms at 2,2′-linkages of the (*Z*,*S*,*Z*,*S*,*Z*,*S*)-structure were −44°, −45°, and −47°, larger than those in the corresponding [6]CNAP counterpart (ca. 30°).[16] The 9,9′-linkages with 8a-9-9′-8a′ carbon atoms exhibited dihedral angles of 59°, 62°, and 62°, comparable to those in [6]cyclo-1,3-pyrene (ca. 60°).[16] Remarkably, two enantiomers of (*Z*,*S*,*Z*,*S*,*Z*,*S*)*-[6]CPhen$_{2,9}$ independently showed one-dimensional alignment of the central nanopores in the crystals. The void volume occupied 30% of the unit cell, making it promisingly applicable toward porous functional materials.[21] Crystallization of a diastereomeric mixture of [4]CPhen$_{2,9}$ afforded single crystals of (*Z*,*S*,*Z*,*R*)-[4]CPhen$_{2,9}$ that were suitable for X-ray crystallographic analysis. As shown in Fig. 5b, (*Z*,*S*,*Z*,*R*)-[4]CPhen$_{2,9}$ showed dihedral angles of −48° and 48° at 2,2′-linkages, and −66° and 66° at 9,9′-linkages. The macrocycles of (*Z*,*S*,*Z*,*R*)-[4]CPhen$_{2,9}$ were packed in a herringbone motif, and the void volume was negligible.

The formation of unexpected [4]CPhen$_{2,9}$ was rationalized by the severe repulsion between hydrogen atoms at the terminal rings of the 1,1′-binaphthyl units. As shown in Fig. S15 in ESI, such steric effects distorted the 9,9′-linkages in [4]CPhen$_{2,9}$, as observed from the angles of 113.2° and 114.4° measured for the 10-9-9′ and 9-9′-10′ carbon atoms, respectively, smaller than those in [6]CPhen$_{2,9}$ (ca. 118.2°), indicating a relief from steric congestion at 1,1′-binaphthyl linkages in [4]CPhen$_{2,9}$.[22, 23] As a result, the constrained tetrameric macrocycle was synthetically viable.

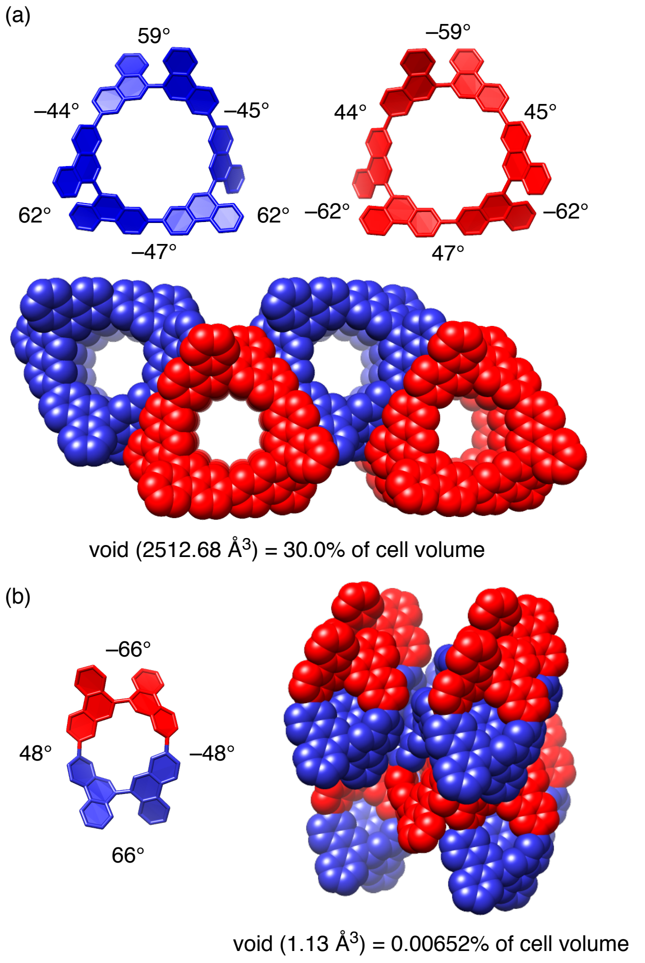

Fig. 5. Crystal structure and packing of (a) (*Z*,*S*,*Z*,*S*,*Z*,*S*)*-[6]CPhen$_{2,9}$ racemate and (b) (*Z*,*S*,*Z*,*R*)-[4]CPhen$_{2,9}$. Hydrogen atoms and solvent molecules are omitted for clarity.

Atropisomerization and racemization

To evaluate the thermal dynamics of [6]CPhen$_{2,9}$, we investigated the isomerization process of (*Z*,*R*,*Z*,*R*,*Z*,*R*)-[6]CPhen$_{2,9}$ in solution at varied temperatures. As shown in Fig. 6a, (*Z*,*R*,*Z*,*R*,*Z*,*R*)-[6]CPhen$_{2,9}$ isomerized to afford other stereoisomers upon heating at 149 °C, and the molar ratio of stereoisomers reached an equilibrium over 16000 min. (*Z*,*R*,*Z*,*R*,*Z*,*S*)-[6]CPhen$_{2,9}$ experienced an initially rapid increase, followed by a steady growth of (*Z*,*S*,*Z*,*S*,*Z*,*R*)-[6]CPhen$_{2,9}$ and a gradual rise of (*Z*,*S*,*Z*,*S*,*Z*,*S*)-[6]CPhen$_{2,9}$ (Fig. 6b), suggesting that (*Z*,*R*,*Z*,*R*,*Z*,*R*)-[6]CPhen$_{2,9}$ was converted first to (*Z*,*R*,*Z*,*R*,*Z*,*S*)-[6]CPhen$_{2,9}$ and subsequently to the others. This result indicated that thermal isomerization proceeded through a stepwise pathway. We then estimated the first-order rate constants k (s^{-1}) of the conversion at various temperatures by virtue of the equation $\ln([x]_t/[x]_0) = -kt$, wherein $[x]_0$ refers to the initial ratio of the integration of (*Z*,*R*,*Z*,*R*,*Z*,*R*)-[6]CPhen$_{2,9}$, whereas $[x]_t$ refers to the ratio of the integration of (*Z*,*R*,*Z*,*R*,*Z*,*R*)-[6]CPhen$_{2,9}$ at time t during the conversion. The Eyring plot of the temperature-dependent decay provided the following activation parameters: $\Delta H^{\ddagger} = +34$ kcal/mol, $\Delta S^{\ddagger} = -4.4$ cal/mol•K and $\Delta G^{\ddagger} = +35$ kcal/mol at 298 K (see Fig. S17,18 in ESI). The energy barrier of the rotation of aromatic panels was larger than those in [8]CPhen$_{3,9}$ ($\Delta H^{\ddagger} = +25$ kcal/mol)[11] and [10]cyclo-1,4-naphthylene ($\Delta H^{\ddagger} = +28$ kcal/mol).[24] We further studied the structures and energetics of thermal isomerization of [6]CPhen$_{2,9}$ by DFT calculations at the B3LYP/6-31G(d,p) level of theory (see Fig. S19 in ESI), and the energy barrier of rotation was calculated to be $\Delta E^{\ddagger} = 35.5$ kcal/mol, which reproduced the experimental value with good agreement. The half-life time was estimated to be $t_{1/2} = 2800$ years at 298 K, indicative of the high configurational rigidity of [6]CPhen$_{2,9}$ at ambient temperature.

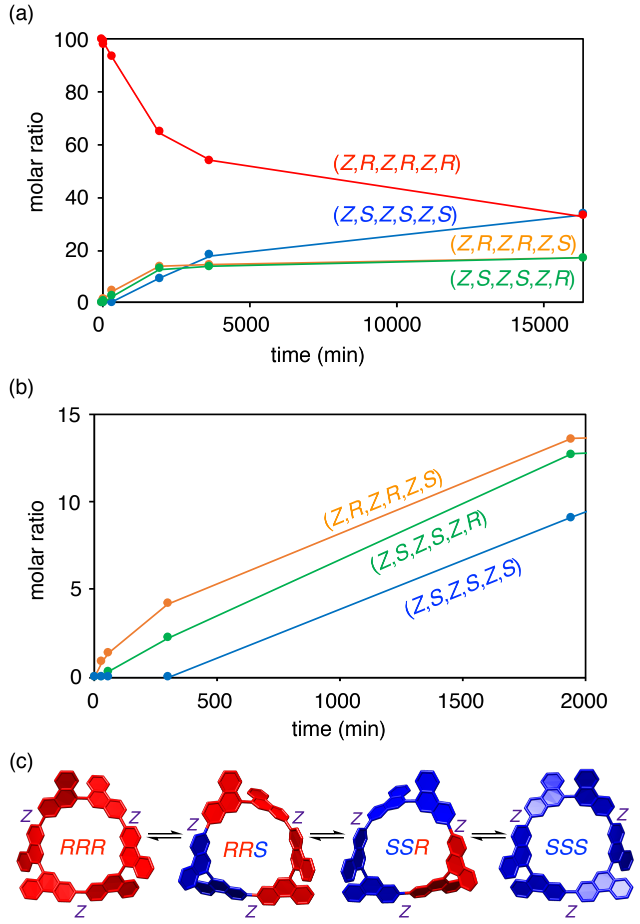

Fig. 6. (a) Time-course analysis of atropisomerization of (*Z*,*R*,*Z*,*R*,*Z*,*R*)-[6]CPhen$_{2,9}$ in 1,2,4-trichlorobenzene at 149 °C. (b) Early-stage atropisomerization of (*Z*,*R*,*Z*,*R*,*Z*,*R*)-[6]CPhen$_{2,9}$. (c) Proposed atropisomerization mechanism of [6]CPhen$_{2,9}$.

Racemization kinetics of (*Z*,*R*,*Z*,*R*)-[4]CPhen$_{2,9}$ were investigated by CD spectroscopy at various temperatures. As shown in Fig. S20–22 in ESI, the racemization process was followed by the decay of the maximum CD signal at 298 nm. The racemization underwent a first-order reaction, and by the equation $\ln([CD]_t/[CD]_0) = -kt$, the rate constant was estimated to be $k = 8.6 \times 10^{-6}$ s^{-1} at 0 °C. The temperature dependence of the rate constant was elucidated with the Eyring equation to provide the energy barriers of $\Delta H^{\ddagger} = +18$ kcal mol^{-1}, $\Delta S^{\ddagger} = -16$ cal/mol•K, and $\Delta G^{\ddagger} = +23$ kcal mol^{-1} at 298 K (see Fig. S23 in ESI). The energy barrier of the rotation of aromatic panels was smaller than those in [8]CPhen$_{3,9}$ ($\Delta H^{\ddagger} = +25$ kcal/mol)[10] and

[10]cyclo-1,4-naphthylene ($\Delta H^{\ddagger}$ = +28 kcal/mol).[21] The half-life time was estimated to be $t_{1/2}$ = 75 min at 298 K, corresponding to the observation that [4]CPhen$_{2,9}$ existed as a diastereomeric mixture after storage for hours at ambient temperature. The reduced energy barrier for the tetrameric macrocycle was likely ascribed to its large ring strain.

Conclusions

We synthesized a novel type of cycloarylene, [*n*]CPhen$_{2,9}$ (*n* = 4, 6 and 8), possessing mixed *E*/*Z*- and *R*/*S*-biaryl linkages through Ni-mediated Yamamoto-type coupling. [6]CPhen$_{2,9}$, the dominant macrocyclic product, theoretically has 20 stereoisomers with 10 diastereomers and 10 enantiomer pairs, of which two diastereomers and two enantiomer pairs were isolated and characterized. The tetrameric counterpart, [4]CPhen$_{2,9}$, was unprecedentedly afforded, possibly due to the steric effect of constrained 1,1′-binaphthyl units. [4]CPhen$_{2,9}$ contains 9 stereoisomers with six diastereomers and three enantiomer pairs, and we separated two diastereomers and one enantiomer pair. These results suggested that *E*/*Z* linkages did not contribute to any experimentally attainable isomer, and the chirality in [*n*]CPhen$_{2,9}$ was derived from the intrinsic axial chirality at *R*/*S* linkages. We separated one isomer of [8]CPhen$_{2,9}$ and determined its structure with conformational search calculations. Scan calculations suggested that the 2,2′-linkages in [*n*]CPhen$_{2,9}$ adopted fixed *Z*- or *E*-configurations, which gave rise to a new class of dynamics of atropisomerism for biaryl linkages. We investigated the dynamic process of the rotation of phenanthrenylene panels in [6]CPhen$_{2,9}$. The isomerization proceeded in a stepwise pathway, and the energy barrier was estimated to be +34 kcal/mol, in good agreement with the value calculated by DFT. Racemization of (*Z*,*R*,*Z*,*R*)-[4]CPhen$_{2,9}$ was studied with variable-temperature CD, which revealed an energy barrier of +18 kcal/mol. The present study consolidated our understanding of *E*/*Z* biaryl linkages.

Conflicts of interest

The authors declare no conflict of interest.

Acknowledgements

This study is partly supported by JST ERATO (JPMJER1301) and KAKENHI (19H02552 and 19K22180). We were granted access to the X-ray diffraction instruments in the SPring-8 BL38B1 and BL26B1 beamlines (nos. 2018B1394 and 2019B1082).

Notes and references

1 (a) R. Adams and H. C. Yuan, *Chem. Rev.*, **1933**, *12*, 261−338; (b) M. Ōki, *The Chemistry of Rotational Isomers*, Springer, New York, **1993**; (c) E. L. Eliel, S. H. Wilen and L. N. Mander, *Stereochemistry of Organic Compounds,* Wiley, Hoboken, **1994**, Chap. 14.

2 R. Kuhn in *Stereochemie* (Ed.: K. Freudenberg), Franz Deuticke, Leipzig, **1933**, pp. 803−824.

3 G. H. Christie and J. Kenner, *J. Chem. Soc., Trans.*, **1922**, *121*, 614−620.

4 R. Noyori and H. Takaya, *Acc. Chem. Res.*, **1990**, *23*, 345−350.

5 (a) R. S. Cahn, C. Ingold and V. Prelog, *Angew. Chem., Int. Ed. Engl.*, **1966**, *5*, 385−415; (b) G. P. Moss, *Pure Appl. Chem.*, **1996**, *68*, 2193−2222.

6 Z. Sun, T. Matsuno and H. Isobe, *Bull. Chem. Soc. Jpn.*, **2018**, *91*, 907−921.

7 In ideal systems, the *R*/*S* stereoisomers with twisted biaryl linkages possess energy barriers of biaryl rotations at dihedral angles of ±180° and 0°, whereas *E*/*Z* stereoisomers possess the barriers at ±90°.

8 S. Hitosugi, W. Nakanishi, T. Yamasaki and H. Isobe, *Nature Commun.*, **2011**, *2*, 492.

9 S. Hitosugi, W. Nakanishi and H. Isobe, *Chem.-Asian J.*, **2012**, *7*, 1550−1552.

10 (a) Z. Sun, P. Sarkar, T. Suenaga, S. Sato and H. Isobe, *Angew. Chem., Int. Ed.*, **2015**, *54*, 12800−12804; (b) Z. Sun, T. Suenaga, P. Sarkar, S. Sato, M. Kotani and H. Isobe, *Proc. Natl. Acad. Sci. USA*, **2016**, *113*, 8109−8114.

11 P. Sarkar, Z. Sun, T. Tokuhira, M. Kotani, S. Sato and H. Isobe, *ACS Cent. Sci.*, **2016**, *2*, 740−747.

12 A. N. Nesmeyanov, T. P. Tolstaya, L. N. Vanchikova and A. V. Petrakov, *Bull. Acad. Sci. USSR, Div. Chem. Sci.*, **1980**, *29*, 1789−1792.

13 We employed Ni-mediated macrocyclization, which have been employed in the synthesis of cyclo-*meta*-arylenes (ref. 14c, 15a, 16 and 17). We noticed that another strategy, Pt-mediated macrocyclization and subsequent reductive elimination, have been employed in the synthesis of cycloarylenes with *E/Z*-biaryl linkages (ref. 7, 9 and 10).

14 Herein we indicated the arylene panels that exhibited a directing angle of 120° between two connecting positions. See ref. 13−16.

15 For cyclo-*meta*-phenylenes and related derivatives, see: (a) H. A. Staab and F. Binnig, *Chem. Ber.*, **1967**, *100*, 293−305; (b)W. Pisula, M. Kastler, C. Yang, V. Enkelmann, K. Müllen, *Chem.-Asian J.*, **2007**, *2*, 51−56; (c) J. Y. Xue, K. Ikemoto, N. Takahashi, T. Izumi, H. Taka, H. Kita, S. Sato and H. Isobe, *J. Org. Chem.*, **2016**, *79*, 9735−9739.

16 For cyclo-2,7-naphthylenes and related derivatives, see: (a)W. Nakanishi, T. Yoshioka, H. Taka, J. Y. Xue, H. Kita and H. Isobe, *Angew. Chem., Int. Ed.*, **2011**, *50*, 5323−5326; (b) W. Nakanishi, J. Y. Xue, T. Yoshioka and H. Isobe, *Acta Crystallogr., Sect. E: Struct. Rep. Online*, **2011**, *E67*, o1762−o1763; (c) J. Y. Xue, W. Nakanishi, D. Tanimoto, D. Hara, Y. Nakamura and H. Isobe, *Tetrahedron Lett.*, **2013**, *54*, 4963−4965.

17 For cyclo-2,7-anthrylenes and related derivatives, see: (a) Y. Yamamoto, K. Wakamatsu, T. Iwanaga, H. Sato and S. Toyota, *Chem.-Asian J.*, **2016**, *11*, 1370−1375; (b) Y. Yamamoto, E. Tsurumaki, K. Wakamatsu and S. Toyota, *Angew. Chem., Int. Ed.*, **2018**, *57*, 8199−8202.

18 For cyclo-1,3-pyrenylenes and related derivatives, see: (a) D. Lorbach, A. Keerthi, T. M. Figueira-Duarte, M. Baumgarten, M. Wagner and K. Müllen, *Angew. Chem., Int. Ed.*, **2016**, *55*, 418−421; (b) K. Ikemoto, S. Sato and H. Isobe, *Chem. Lett.*, **2016**, *45*, 217−219.

19 An asterisk indicated the presence of an enantiomeric pair (*vide infra*).

20 V. I. Minkin, *Pure Appl. Chem.*, **1999**, 71, 1919−1981.

21 (a) S. Sato, A. Unemoto, T. Ikeda, S. Orimo and H. Isobe, *Small*, **2016**, *12*, 3381−3387; (b) H. Sakamoto, T. Fujimori, X. Li, K. Kaneto, K. Kan, N. Ozaki, Y. Hijikata, S. Irle and K. Itami, *Chem. Sci.*, **2016**, *7*, 4204−4210; (c) N. Ozaki, H. Sakamoto, T.

Nishihara, T. Fujimori, Y. Hijikata, R. Kimura, S. Irle and K. Itami, *Angew. Chem., Inti. Ed*, **2017**, *56*, 11196−11202; (d) J. M. Van Raden, E. J. Leonhardt, L. N. Zakharov, A. Pérez-Guardiola, A. J. Pérez-Jiménez, C. R. Marshall, C. K. Brozek, J. C. Sancho-García and R. Jasti, *J. Org. Chem*, **2020**, *85*, 129−141.

22 M. T. Ashby, G. N. Govindan and A. K. Grafton, *J. Am. Chem. Soc.*, **1994**, *116*, 4801−4809.

23 The smaller angles at 10-9-9′ and 9-9′-10′ dihedrals may allow phenanthrenylene panels to relief at wider, less hindered dihedrals.

24 K. Okada, A. Yagi, Y. Segawa and K. Itami, *Chem. Sci.*, **2017**, *8*, 661−667.

Graphical Abstract

A novel series of cycloarylenes with blended *E*/*Z* and *R*/*S* linkages was synthesized, and their cyclostereoisomerism were elaborated.

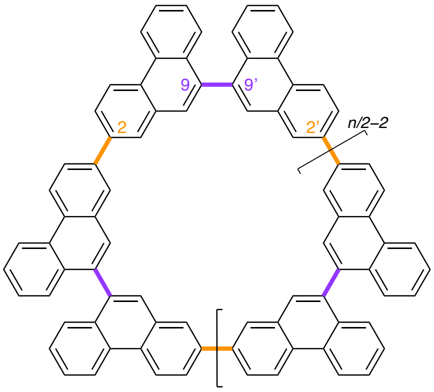

[*n*]CPhen$_{2,9}$ (*n* = 4, 6 and 8)

2,2'-linkages: fixed *E*/*Z*-configuration

9,9'-linkages: rigid *R*/*S*-configuration